

Structural Properties of Tetra-*tert*-butyl Zinc(II) Phthalocyanine Isomers on a Au(111) Surface

Z. T. Deng, H. M. Guo, W. Guo, L. Gao, Z. H. Cheng, D. X. Shi, and H.-J. Gao*

Beijing National Laboratory for Condensed Matter Physics, Institute of Physics, Chinese Academy of Sciences, P.O. Box 603, Beijing 100190, People's Republic of China

Received: February 9, 2009; Revised Manuscript Received: May 14, 2009

The self-assembly behavior of the mixture of tetra-*tert*-butyl zinc(II) phthalocyanine (TB-ZnPc) isomers on a Au(111) surface has been investigated by means of scanning tunneling microscopy (STM). Four *tert*-butyl groups are added to four peripheral benzene rings of zinc(II) phthalocyanine, which gives the planar molecules a three-dimensional structure. Two possible substituting locations for each *tert*-butyl group result in a mixture of structural isomers, which are easily identified by STM. Two different structures have been distinguished in the monolayer regime depending on the preparation procedure. One is a quasi-ordered structure whereby the molecules are arranged in the closest-packed way, and the second is an ordered structure in which the molecules are arranged side by side. The more ordered molecular network in the latter is considered to be a consequence of unification of TB-ZnPc isomers.

I. Introduction

Understanding and controlling the molecular architectures in self-assembled monolayers (SAM) is an important concern for their applications, e.g., in molecular electronics and optoelectronics devices.^{1,2} Recently, attention has been focused on fabricating a functional molecular monolayer by the intermolecular noncovalent interaction on different single-crystalline metal substrates.^{3–7} The self-assembly of a multiple-component mixture of molecules on substrate has been investigated to obtain various functional, interfacial structures.^{8,9} Therein, functional molecules with structural isomers, coexisting with each other, are particularly important and interesting due to the effect of their different structures and configurations on the self-assembly regime.

The molecular configurations of different isomers on the surface can be identified by scanning tunneling microscopy techniques (STM), which has the capability of accessing signals of a single molecule at a subnanometer scale. For example, STM has determined the conformational changes of the substituent angle of a single porphyrin derivative molecule. Moreover, the conformation can be modified by further applying additional force with the STM tip.¹⁰ Different molecular isomers have been distinguished in their self-assembling structures on metal surfaces by STM imaging.^{11,12} However, the aggregation and structural evolution of functional molecules with structural isomers during their self-assembling process on substrate has rarely been investigated. The mechanism of self-assembly and structural evolution of isomers is still not well understood.

Phthalocyanines (Pcs) and their derivatives have attracted special interest because of many applications in the areas of gas-sensing devices, photovoltaic applications, light-emitting diodes, organic field effect transistors, pigments and dyes, etc. The tetra-*tert*-butyl zinc(II) phthalocyanine (TB-ZnPc) is an ideal candidate molecule to investigate the noncovalent interactions controlled configuration transformation in self-assembly monolayer. Four *tert*-butyl (*t*Bu) groups are added to four

periphery benzene rings of zinc(II) phthalocyanine, which gives the planar molecules a three-dimensional structure. *tert*-Butyl groups, widely used as a substituent to design functional molecules, can enhance the solubility, chemical stability, and light fastness of organic molecules.¹³ In our recent work, we showed single (*t*Bu)₄-ZnPc molecules can thermally rotate around the nitrogen–gold adatom bond, which is the fix point on the surface since the lateral motion of the molecule is blocked by the gold adatom, and then regular arrays of anchored molecular rotors were successfully constructed on a Au(111) surface.¹⁴

In this paper, we report the scanning tunneling microscopy (STM) investigation on the initial adsorption configuration and self-assembled monolayer of TB-ZnPc isomers on Au(111). The four isomers of TB-ZnPc molecules, which come from two possible substituting locations of each *t*Bu group, are easily identified by STM observation. Furthermore, two different monolayer structures can be obtained depending on the substrate temperature. With increasing substrate temperature, the ordering and packing density of the TB-ZnPc monolayer increases. An ordered structure is formed while the molecule–substrate interaction remains fairly constant. This behavior is attributed to the deformation of phthalocyanine skeletons and the twisting of the *t*Bu groups. The new molecular self-assembly process provides a new train of thought in fabricating molecular electronics and optoelectronic devices with structural isomers.

II. Experimental Details

Sample preparation and investigation were carried out in a combined ultra-high-vacuum (UHV) molecular beam epitaxy (MBE) and low-temperature scanning tunneling microscopy (LT-STM) system. The background pressure is in the range of 10^{−10} mbar. Prior to the adsorption experiment, the gold single crystal is cleaned by repeated cycles of Ar⁺ sputtering (1 keV, 30 min) and subsequent annealing at 800 K (20 min). The bare gold surface is imaged before dosing to confirm its cleanliness. The TB-ZnPc molecules (synthesized by Liu et al., IOC, CAS) are evaporated from a crucible heated to 530 K. This results in

* To whom correspondence should be addressed. E-mail: hjgao@iphy.ac.cn.

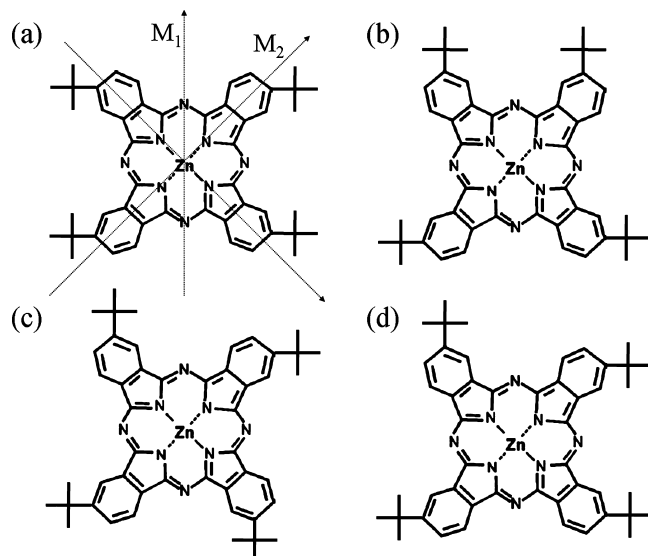


Figure 1. (a–d) Chemical structure formulas of four isomers of TB-ZnPc molecules. M_1 and M_2 are the symmetry mirrors of the phthalocyanine skeleton of the molecule.

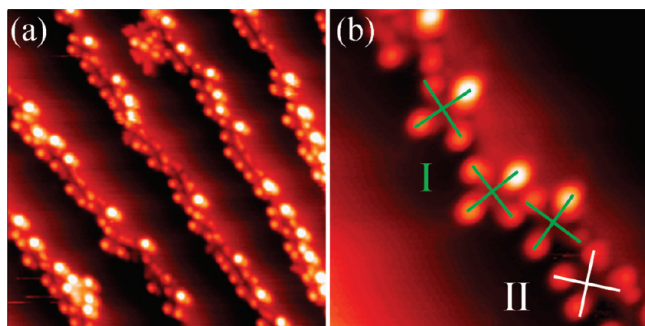


Figure 2. (a) STM image of the initial growth stage of TB-ZnPc on Au(111). Every molecule is adsorbed at the step edge. $U_{\text{bias}} = -1.3$ V, $I_t = 50$ pA, 25 nm \times 25 nm. (b) Details of the adsorption configuration of molecules at the step edge. The crosses with different color mark a different adsorption conformation. $U_{\text{bias}} = -0.5$ V, $I_t = 60$ pA, 9 nm \times 9 nm.

a deposition rate of about 0.03 monolayer (ML) per minute. By changing the surface temperature and deposition time, molecule layers of different coverage are prepared and the entire growth process of the TB-ZnPc monolayer is investigated by means of LT-STM. The low temperature of 4.5 and 77 K greatly reduces the mobility of TB-ZnPc molecules on Au(111), and details of the molecules can be observed.

III. Results and Discussions

A. Single-Molecule Adsorption of Different Isomers. Figure 1 gives the chemical structure of the TB-ZnPc molecule, in which four of the eight periphery hydrogen atoms in the phenyl rings are substituted by four *t*Bu groups. All four *t*Bu groups have two possible substituting locations. Taking symmetry into account, this leads to four different isomers of TB-ZnPc, as shown in Figure 1a–d. The choice of TB-ZnPc, with its nonbonding Zn 3d band, and Au(111), a surface of low energy, should in principle result in a low molecule–substrate interaction.

When the molecules are deposited onto a clean surface, usually the locations with the lowest adsorption energy such as steps, kinks, and flaws on the terrace will be the optimized adsorption sites. As shown in Figure 2a, at the initial stage, all TB-ZnPc molecules are adsorbed at the step edge, where each

molecule is imaged as four bright spots. The bright features can be attributed to the *t*Bu groups substituted benzene rings in a TB-ZnPc molecule with a flat-lying orientation. The central zinc ions appear as a dark area. The close-up image in Figure 2b clearly suggests two different adsorption configurations. Configuration I, marked by green crosses, has one leg on the upper terrace, one leg on the lower terrace, and the other two legs on the boundary edge. In configuration II, marked by a white cross, two legs are located on the upper terrace and the other two on the lower.

When the step edges are fully occupied, the molecules start to adsorb first on the elbow positions, then on the fcc and hcp regions of the Au(111) surface.¹⁵ Some individual molecules can be observed keeping their original configuration at liquid helium (LHe) temperature, while at higher temperature (liquid nitrogen temperature, 77 K) they will diffuse or rotate on the Au surface. As shown in Figure 3, four isomers of TB-ZnPc can be distinguished by the STM imaging at LHe temperature. A rectangle, trapezoid, square, and trapezium are used to represent the four isomers according to their shape observed in the STM images. Between two adjacent bright spots of each molecule, three typical length are measured (see Figure 3a–d), corresponding to three distances between two adjacent *t*Bu groups. The shape of the four molecules is indicated in each STM image. Lines with three different lengths, 1.4, 1.25, and 1.0 nm, assemble to the four symbols. The apparent height of the molecule is about 1 Å, a value in accordance with those of other MPCs recorded in a flat-lying configuration.

B. Structural Evolution in the Monolayer. Figure 4a shows an STM image of one kind of TB-ZnPc isomer, in which one single molecule and one dimer are observed. To achieve the most stable configuration and the lowest adsorption energy, the molecules in the dimer are not arranged in a side-by-side configuration. Instead, the long axes of the two molecules are perpendicular to each other, and the *t*Bu groups are in close contact with the *t*Bu groups in the neighboring molecule.

With the increasing coverage, the molecules are arranged in a similar way to build two-dimensional structures. A molecular monolayer is shown in Figure 4b, which is recorded after depositing TB-ZnPc molecules on Au(111), while the surface was kept at 80 °C. This TB-ZnPc isomer arrangement is noted by the P_1 structure, giving a packing density of 0.31 molecule/nm². The closest-packing way of this TB-ZnPc molecular arrangement is also the most common molecular arrangement of metal phthalocyanines.^{16–18} From the STM images, one can obtain the lattice parameters: $A_1 = 1.78$ nm, $B_1 = 1.82$ nm, and an angle of 90° between the basis vectors. Besides, the angle between the basis vector A_1 and the^{1–10} direction of the Au(111) substrate is about 25°. Due to the different conformation of isomers, the molecular monolayer is not perfectly ordered. In other words, P_1 is a quasi-ordered monolayer. The two TB-ZnPc isomers marked by two yellow circles can be identified with the trapezium shapes but different orientations. Other isomers can also be observed from the monolayer, such as a square-shaped TB-ZnPc molecule, which is marked by a green circle.

Figure 4c shows a large-scale landscape of TB-ZnPc self-assembled monolayer with P_1 structure. The formation of large well-ordered domains extended over hundreds of nanometers indicates a low diffusion barrier of TB-ZnPc on Au(111). The molecules in the first layer exhibit a saturated and stable structure, and few individual molecules are adsorbed on the first layer. Due to the various environments, the molecules in the second layer are imaged differently as irregular bright spots.

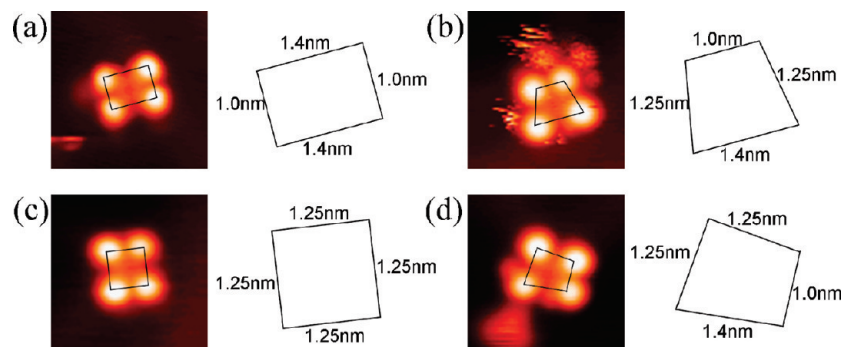


Figure 3. Occupied state STM images of TB-ZnPc isomers on Au(111). The chemical formulas of isomers shown in a–d have been presented at Figure 1a–d with the same sequence. The shape of the isomers is represented by the symbols next to the STM images. The size of each symbol is determined from the distance between the center of two adjacent bright lobes of each isomer. Image sizes: 5 nm \times 5 nm.

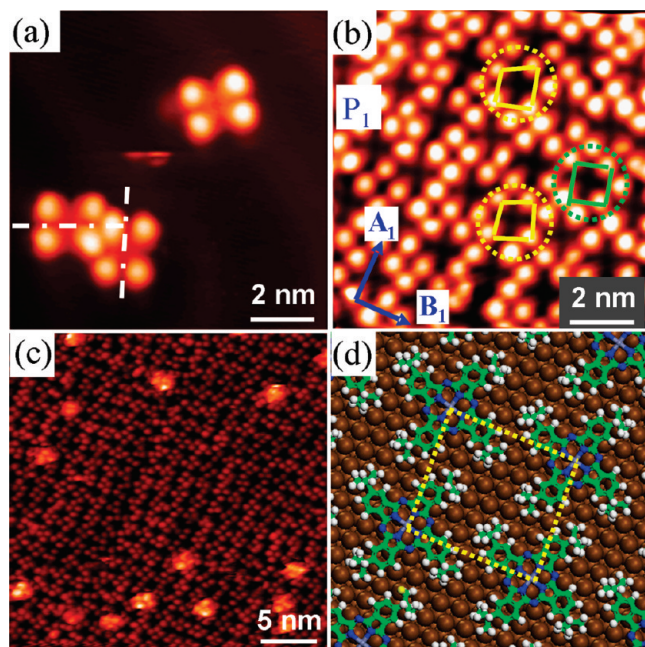


Figure 4. (a) High-resolution STM image of a single molecule and dimer. All molecules are imaged as four bright spots with D_{2h} symmetry. $U_{\text{bias}} = -1.8$ V, $I_t = 50$ pA. (b) Monolayer of TB-ZnPc molecules adsorbed on Au(111) at 80 °C (Structure P1). The lattice parameters are $A_1 = 1.78$ nm, $B_1 = 1.82$ nm, and $\gamma_1 = 90^\circ$. The yellow and green circles mark two different isomers with different trapezium shapes. $U_{\text{bias}} = -0.8$ V, $I_t = 36$ pA. (c) Large-scale image of the TB-ZnPc monolayer. $U_{\text{bias}} = -1.26$ V, $I_t = 36$ pA. (d) Proposed model for the TB-ZnPc P1 structure; one unit cell is marked by the dashed yellow lines.

Figure 4d gives a possible model to illustrate the molecular arrangement of the first layer in the P1 structure. Only one kind of TB-ZnPc isomer is shown as an example. On the basis of a unit cell deduced from Figure 4d, the molecules are placed at a position with most of the atoms in the TB-ZnPc molecule on top of hollow sites of the Au(111) surface. In this model, every *t*Bu group is located in the middle of two groups of the neighboring molecules.

When depositing TB-ZnPc molecules on Au(111) with the substrate temperature increased to 100 °C, a more ordered molecular network P2 rather than P1 will form. Figure 5a shows a large-scale landscape of the P2 network structure. Two domains of P2 network are visible in Figure 5a, which are labeled D_a and D_b. In the middle right of this STM image there is a typical spiral dislocation of Au(111) substrate, which separates D_a into two parts. Note that the ordered molecular arrangement is not affected by the dislocation, which indicates the high stability

of the P2 structure. Disordered regions of the TB-ZnPc monolayer are also seen at the upper left part and lower part in Figure 5a, which suggests a thermodynamic equilibrium between the ordered phase and disordered phase at elevated substrate temperature. The angle between the basis vectors of domain D_a and D_b is 30°. Due to the 6-fold symmetry of the Au(111) surface, the molecular configuration has three equivalent orientations. Because the molecules are able to be arranged side by side along two directions which are parallel with the two mirror axes M1 (see Figure 1a), six equivalent domains can be formed together with the same set of basis vectors. Comparing P1 with P2, the two basis vectors of P1 are perpendicular to each other and the arrangement of molecules along the two vectors is the same. Therefore, only three P1 domains exist on Au(111).

Figure 5b shows a high-resolution image giving the submolecular details of domain D_a. The packing density of molecules in the P2 structure can be counted as 0.35 molecule/nm². Contrary to the molecules in P1, the observed configurational diversity of different isomers decreases greatly. Most of the molecules are imaged as four bright spots arranged in a square shape. The molecules are ordered side by side along one direction which is parallel to one of the unit cell vectors of the monolayer. Along the other basis direction, the molecules are in interlaced arrangements. We describe this TB-ZnPc structure by a unit cell with a molecule in every corner. For the STM images, one can obtain the average lattice parameters: $A_2 = 1.75$ nm, $B_2 = 1.65$ nm, and an angle 75° between the basis vectors. The angle between the A₂ direction and the [1–10] direction of the Au(111) surface is 15°. For all the domains investigated by STM, the mirror axis M1 of the MPc core is aligned along one close-packed direction of the substrate.

We propose a model to interpret the STM image of TB-ZnPc on the Au(111) surface. A TB-ZnPc isomer with a square shape is placed into a unit cell determined from Figure 5b. We chose several possibly stable adsorption configurations of TB-ZnPc on Au(111).¹⁶ After that, we search the most optimized configuration in the monolayer by means of first-principles calculations based on density functional theory (DFT) (for technical details, see ref 19). The result is shown in Figure 5c. The zinc atom is located on the hollow site of Au(111), and the mirror plane M₂ of TB-ZnPc molecule is nearly parallel to a main direction of the Au(111) surface. We also calculate the partial charge density of the TB-ZnPc molecules, which are placed on a unit cell determined from Figure 5b, as shown in Figure 5d and 5e. The calculated images of the partial charge density are in agreement with the STM images of the TB-ZnPc molecules. The four lobes correspond to the four *t*Bu groups

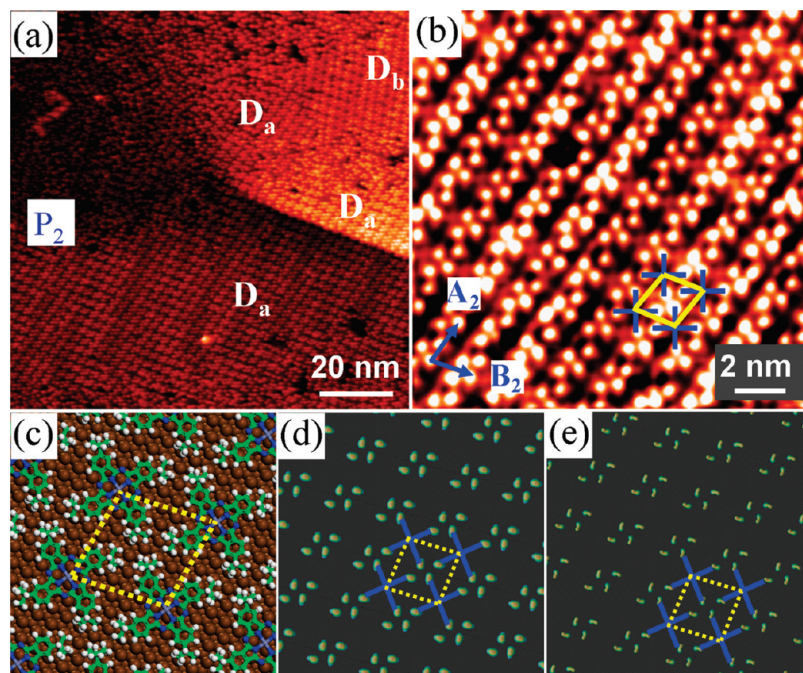


Figure 5. STM image of TB-ZnPc molecules adsorbed on Au(111) at 100 °C (Structure P₂). (a) Large-scale image showing different structural domains. D_a and D_b correspond to two of the six possible domains. $U_{\text{bias}} = -1.2$ V, $I_t = 50$ pA. (b) Enlarged image of domain I shows the high-resolution details, and the lattice parameters are $A_2 = 1.75$ nm, $B_2 = 1.65$ nm, and $\gamma_2 = 75^\circ$. The blue cross lines indicate the molecule, and the yellow lines mark one unit cell in the lattice. $U_{\text{bias}} = -1.2$ V, $I_t = 965$ pA. (c) Ground-state adsorption configuration of the TB-ZnPc molecule on the Au (111) surface. (d and e) Partial charge density of the TB-ZnPc monolayer deposited on the Au(111) surface from the Fermi level to -2 and $+2$ eV, respectively.

and four benzene rings. The darkness in the center of the molecules is attributed to the fully filled 3d orbital of zinc atoms²² and the decoupling of the Pcs skeleton from the Au(111) surface after the molecules are raised by the *t*Bu groups.

Note that the P₁ structure is closest packed in the way of common phthalocyanine monolayers, but its packing density is lower than that of the P₂ structure. This is contrary to common sense because usually the closest-packed structure has the highest density and is well ordered of molecules. From the STM image, Figure 4c, many TB-ZnPc isomers can be observed with different shapes. Due to the influence of different shapes and the compositional disorder of TB-ZnPc isomers, the molecular density of P₁ is lower than P₂, although the molecules are in the closest-packed configuration for Pcs. To explain the contradiction, we propose an isomers unification mechanism. For phthalocyanines and their derivatives, deformation of phthalocyanine skeletons often occurs, only if there are enough molecule–molecule or molecule–substrate interactions.^{23,24} At higher surface temperature, molecules have more energy to overcome potential barriers that result in higher molecular diffusivity. In this regime, the thermodynamic growth mode plays a more dominant role to form more ordered and stable structures. Considering the small thermal energy difference between the P₁ and P₂ structures, we can conclude that the unification process would be explained by deformation of phthalocyanine skeletons and twist of *t*Bu groups other than isomerization of TB-ZnPc isomers. During the self-assembly process of TB-ZnPc molecules when surface kept at 100 °C, the inner rings of *Pc* macrocycles are able to transform into a suitable configuration to adjust the positions of four benzene rings and reduce the difference between four kinds of TB-ZnPc isomers. As shown in Figure 5b, most of the molecules are close to a square shape. The assembled square-shaped molecules can combine more molecules in the same area than assembly of differently shaped molecular isomers.

For each molecule in P₂, each of the two *t*Bu groups is placed closely side by side with two *t*Bu groups of the adjacent molecule. This arrangement of P₂ gives a stronger interaction for deformation than the intramolecule interaction in the P₁ structure, where the *t*Bu groups of the molecules are inserted into the middle of the two *t*Bu groups of another molecule. It is reasonable to conclude that isomers unification is more favorable in the side-by-side arrangement of P₂ than in the interlaced arrangement of P₁. In general, the interlaced arrangement has the highest molecular density for *Pcs* and their derivatives. Therefore, in the P₂ structure, molecules are placed side by side along one direction to achieve the necessary deformation motive and interlaced along another direction for close packing.

IV. Conclusions

We investigated the adsorption configurations and assembly behavior of TB-ZnPc molecules on the Au(111) surface by means of low-temperature STM and DFT calculations. The four isomers of TB-ZnPc molecules can be identified with different shapes from their STM images. In the initial adsorption stage, selective aggregation of TB-ZnPc isomers is observed. In the closest-packed P₁ structure of the TB-ZnPc monolayer, isomers are mixed together and the structure ordering is influenced by the different shapes and compositional disorder of isomers. By raising the substrate temperature during the self-assembly procedure, the *Pc* skeletons have enough energy to deform and most of the TB-ZnPc molecules transform to a square shape. The intermolecular interaction is responsible for the molecular deformation, and another structure P₂ of the self-assembled monolayer can be formed. This investigation is helpful for a deep and comprehensive understanding on the adsorption and growth behavior of TB-ZnPc and other MPc molecules with different isomers.

Acknowledgment. This work was funded by the Natural Science Foundation of China (NSFC, grant nos. 60771037 and 10774176), the National 973 projects of China (no. 2006CB921305), and the Supercomputing Center, CNIC, CAS. We thank S. Rauschenbach and S. Stepanow for helpful discussions.

References and Notes

- (1) Yokoyama, T.; Yokoyama, S.; Kamikado, T.; Okuno, Y.; Mashiko, S. *Nature* **2001**, *413*, 619.
- (2) Dmitriev, A.; Lin, N.; Weckesser, J.; Barth, J. V.; Kern, K. *J. Phys. Chem. B* **2002**, *106*, 6907.
- (3) Shi, D. X.; Ji, W.; Lin, X.; He, X. B.; Lian, J. C.; Gao, L.; Cai, J. M.; Lin, H.; Du, S. X.; Lin, F.; Seidel, C.; Chi, L. F.; Hofer, W. A.; Fuchs, H.; Gao, H.-J. *Phys. Rev. Lett.* **2006**, *96*, 226101. (a) Du, S. X.; Gao, H.-J.; Seidel, C.; Tsetseris, L.; Ji, W.; Kopf, H.; Chi, L. F.; Fuchs, H.; Pennycook, S. J.; Pantelides, S. T. *Phys. Rev. Lett.* **2006**, *97*, 156105. (b) Deng, Z. T.; Lin, H.; Ji, W.; Gao, L.; Lin, X.; Cheng, Z. H.; He, X. B.; Lu, J. L.; Shi, D. X.; Hofer, W. A.; Gao, H.-J. *Phys. Rev. Lett.* **2006**, *96*, 156102.
- (4) Wang, Y. L.; Gao, H.-J.; Guo, H. M.; Wang, S. W.; Pantelides, S. T. *Phys. Rev. Lett.* **2005**, *94*, 106101.
- (5) Gao, L.; Ji, W.; Hu, Y. B.; Cheng, Z. H.; Deng, Z. T.; Liu, Q.; Jiang, N.; Lin, X.; Guo, W.; Du, S. X.; Hofer, W. A.; Xie, X. C.; Gao, H.-J. *Phys. Rev. Lett.* **2007**, *99*, 106402.
- (6) Shi, D. X.; Song, Y. L.; Zhang, H. X.; Jiang, P.; He, S. T.; Pang, S. J.; Gao, H.-J. *Appl. Phys. Lett.* **2000**, *77*, 3203. (a) Shi, D. X.; Song, Y. L.; Zhu, D. B.; Zhang, H. X.; Xie, S. S.; Pang, S. J.; Gao, H.-J. *Adv. Mater.* **2001**, *13*, 1103. (b) Feng, M.; Gao, L.; Deng, Z. T.; Ji, W.; Guo, X. F.; Du, S. X.; Shi, D. X.; Zhang, D. Q.; Zhu, D. B.; Gao, H.-J. *J. Am. Chem. Soc.* **2007**, *129*, 2204. (c) Feng, M.; Guo, X. F.; Lin, X.; He, X. B.; Ji, W.; Du, S. X.; Zhang, D. Q.; Zhu, D. B.; Gao, H.-J. *J. Am. Chem. Soc.* **2005**, *127*, 15338.
- (7) Ma, L. P.; Song, Y. L.; Gao, H.-J.; Zhao, W. B.; Chen, H. Y.; Xue, Z. Q.; Pang, S. J. *Appl. Phys. Lett.* **1996**, *69*, 3752. (a) Gao, H.-J.; Xue, Z. Q.; Wang, K. Z.; Wu, Q. D.; Pang, S. J. *Appl. Phys. Lett.* **1996**, *68*, 2192. (c) Gao, H.-J.; Sohlberg, K.; Xue, S. M.; Ma, L. P.; Fang, X. W.; Pang, S. J.; Pennycook, S. J. *Phys. Rev. Lett.* **2000**, *84*, 1780.
- (8) Hipps, K. W.; Scudiero, L.; Barlow, D. E.; Cooke, M. P. *J. Am. Chem. Soc.* **2002**, *124*, 2126.
- (9) Langner, A.; Tait, S. L.; Lin, N.; Rajadurai, C.; Ruben, M.; Kern, K. *Proc. Natl. Acad. Sci.* **2007**, *104*, 17927–17930.
- (10) Jung, T. A.; Schlittler, R. R.; Gimzewski, J. K. *Nature* **1997**, *386*, 696. (a) Moresco, F.; Meyer, G.; Rieder, K.-H.; Tang, H.; Gourdon, A.; Joachim, C. *Phys. Rev. Lett.* **2001**, *86*, 672.
- (11) Suzuki, H.; Miki, H.; Yokoyama, S.; Mashiko, S. *J. Phys. Chem. B* **2003**, *107* (15), 3659.
- (12) Böhlinger, M.; Morgenstern, K.; Schneider, W.-D.; Berndt, R.; Mauri, F.; Vita, A.; Car, R. *Phys. Rev. Lett.* **1999**, *83*, 324. (a) Böhlinger, M.; Morgenstern, K.; Schneider, W.-D.; Berndt, R. *Angew. Chem., Int. Ed.* **1999**, *38*, 821.
- (13) Perry, J. W.; Mansour, K.; Lee, I.-Y. S.; Wu, X.-L.; Bedworth, P. V.; Chen, C.-T.; Ng, D.; Marder, S. R.; Miles, P.; Wada, T.; Tian, M.; Sasabe, H. *Science* **1996**, *273*, 1533.
- (14) Gao, L.; Liu, Q.; Zhang, Y. Y.; Jiang, N.; Zhang, H. G.; Cheng, Z. H.; Qiu, W. F.; Du, S. X.; Liu, Y. Q.; Hofer, W. A.; Gao, H.-J. *Phys. Rev. Lett.* **2008**, *101*, 197209.
- (15) Cheng, Z. H.; Gao, L.; Deng, Z. T.; Jiang, N.; Liu, Q.; Shi, D. X.; Du, S. X.; Guo, H. M.; Gao, H.-J. *J. Phys. Chem. C* **2007**, *111*, 9240. (a) Cheng, Z. H.; Gao, L.; Deng, Z. T.; Liu, Q.; Jiang, N.; Lin, X.; He, X. B.; Du, S. X.; Gao, H.-J. *J. Phys. Chem. C* **2007**, *111*, 2656.
- (16) Lu, X.; Hipps, K. W.; Wang, X. D.; Mazur, U. *J. Am. Chem. Soc.* **1996**, *118*, 7197.
- (17) Koudia, M.; Abel, M.; Maurel, C.; Bliet, A.; Catalin, D.; Mossoyan, M.; Mossoyan, J.-C.; Porte, L. *J. Phys. Chem. B* **2006**, *110*, 10058.
- (18) Lackinger, M.; Hietschold, M. *Surf. Sci.* **2002**, *L619*, 520.
- (19) Ab initio density functional theory (DFT) calculations are carried out with the Vienna Ab-initio Simulation Package (VASP).²⁰ The generalized gradient approximation (GGA) according to Perdew–Burke–Ernzerhof (PBE)²¹ for exchange–correlation potential, Projector Augmented Waves (PAW), and a plane wave basis set as implemented in the VASP are used. The Au(111) supercells are modeled by a three-layer Au film with TB-ZnPc molecules adsorbed on only one side of the surface. This geometry is justified in view of the very low adsorption energies and, consequently, low hybridization of electronic states, which does not give rise to surface dipoles. A vacuum of at least 12 Å is used to separate the mirror images in the *z* direction. The energy cutoff for plane waves is 520 eV. Due to numerical limitations and the size of the system the surface Brillouin zone was sampled with the Γ point only. In structural relaxations, all atoms except for the bottom Au layers were fully relaxed until the net force on every atom was smaller than 0.02 eV/Å.
- (20) Kresse, G.; Hafner, J. *Phys. Rev. B* **1993**, *47*, 558. (a) Kresse, G.; Furthmüller, J. *Phys. Rev. B* **1996**, *54*, 16697.
- (21) Perdew, J. P.; Chevary, J. A.; Vosko, S. H.; Jackson, K. A.; Pederson, M. R.; Singh, D. J.; Fiolhais, C. *Phys. Rev. B* **1992**, *43*, 6671.
- (22) Yoshimoto, S.; Tsutsumi, E.; Suto, K.; Honda, Y.; Itaya, K. *Chem. Phys.* **2005**, *319*, 147.
- (23) Qiu, X. H.; Nazin, G. V.; Ho, W. *Phys. Rev. Lett.* **2002**, *92*, 206102.
- (24) Fukuda, T.; Homma, S.; Kobayashi, N. *Chem.—Eur. J.* **2005**, *11*, 5205.

JP901193H